SAFE OPERATIONAL BANDWIDTH OF GAS STORAGE RESERVOIRS
WP1 REPORT

Massimiliano Ferronato
Andrea Franceschini
Giovanni Isotton
Carlo Janna
Pietro Teatini
Omar Tosatto
Claudia Zoccarato

Padova, January 31, 2018

DIPARTIMENTO DI INGEGNERIA CIVILE, EDILE E AMBIENTALE - I C E A
DEPARTMENT OF CIVIL, ENVIRONMENTAL AND ARCHITECTURAL ENGINEERING

Contents

1. Introduction

The project 'Safe operational bandwidth of gas storage reservoirs' is aimed at investigating the geomechanical hazards and risks associated with gas storage in Underground Gas Storage (UGS) reservoirs. In particular, it is focused on the geomechanical processes that can be responsible for unexpected seismicity because of fault slippage in and around the storage reservoirs due to UGS activities.

A summary of WP1 activities is provided in this report. A bibliographic review of the most recent scientific publications has been carried out to develop an inventory of possible mechanisms of fault reactivation induced by fluid injection/production into/from deep reservoirs. Seismic occurrences are subdivided according to the reservoir development stage (primary production, cushion gas injection, and UGS), the event focal mechanism and magnitude ($M \leq 1$, $1 < M < 3$, and $M \geq 3$), and the hypocenter location with respect to the developed formation (below, at the same depth, above). Moreover, the recorded seismic events are associated to the hydro-geomechanical and mineralogical properties of the reservoir formation, the fault geometry, the natural stress regime, the presence and quality of the monitoring seismic network.

The analysis is primarily focused on UGS plants where seismic activity has been recorded, but also on producing reservoirs where injection operations induced or triggered (micro-) seismicity. In particular, cases where *unexpected seismicity* occurred are selected to possibly identify the factors that fall beyond the well-known causes for fault re-activation, e.g., at peak depletion/minimum reservoir pressure.

The available scientific literature on UGS seismicity is relatively scarce, with a few main occurrences detected, investigated and publicly released worldwide. The main examples include the UGS sites of Norg, Grijpskerk and Bergermeer in The Netherlands and the Castor UGS project in Spain. Additional information on possible fault activation and consequent unexpected seismicity is found in the Duvernay Formation (Alberta, Canada). A summary on UGS case studies in Italy is also provided, although no seismic events have been associated to this activity till now. Cases of seismic events recorded in geothermal fields and waste water injection are disregarded in this context because the mechanisms of fault (re-) activation are unlikely to occur in UGS reservoirs. Recent examples cited in the literature are anyway included in a summary table for the sake of completeness.

2. Bibliographic analysis

2.1 "Unexpected" seismic occurrences

An extensive literature search has been carried out to investigate the state-of-the-art knowledge on the key mechanisms for induced seismicity in UGS plants. Few cases only of UGS seismicity are published in literature, being mainly related to sites in The Netherlands and to the Castor project in Spain. A more detailed analysis focusses on the mentioned cases, with an additional study of unexpected seismicity in Canada.

The inventory is summarized in Tables 1 and 2. The reservoirs and the recorded seismicity are categorized according to the reservoir development stage, the event focal mechanism and magnitude, and the hypocenter location with respect to the developed formation and the fault geometry (Table 1). Moreover, the recorded seismic events are associated to the hydro-geomechanical and mineralogical properties of the reservoir formation, the natural stress regime, the presence and quality of the monitoring seismic network, and the production history (Table 2).

The tables are meant to identify the main properties of the investigated sites and compare the occurrences to delineate common factors or key differences. An in-depth analysis of the inventory cases is also provided in this section for a deeper comprehension of the reservoirs that is fundamental to delineate the possible fault mechanisms in the next work package.

Table 1 Inventory of induced seismicity cases according to reservoir development stage, event focal mechanism and magnitude, and hypocenter location with respect to the developed formation and the fault geometry. PP=primary production; UGS=underground gas storage; CG=cushion gas; PT=post-treatment; HF=hydraulic fracturing.

RESERVOIR	LOCATION	TYPE	STAGE	ACTIVATED FAULT GEOMETRY	DEPTH			MAGNITUDE		
					below	reservoir	above	≤1	1 - 3	≥3
Norg	The Netherlands	UGS	PP; UGS	Slip motion on a sub-vertical NW-SE fault (PP) and a sub-vertical compressive SW-NE fault (UGS)		x			x (2)	
Grijpskerk	The Netherlands	UGS	UGS	large uncertainty to locate active faults					x (2)	
Bergermeer	The Netherlands	UGS	PP;CG;UGS	strike: SSW; dip: 60-65		x		x (1 - CG)		x (4 - PP)
Duvernay Formation	Canada	HF	PT	strike-slip motion on subvertical, ~-S/E-W oriented faults	x	x			x	x (4.1)
Castor	Spain	UGS	PT	secondary fault was activated during the 2013 earthquake sequence instead of the Amposta fault	x	x			x	x (4.3)

Table 2 Inventory of induced seismicity cases according to the natural stress regime of the reservoir formation, the presence and quality of the monitoring seismic network, the properties of the reservoir formation, and the production history. PP=primary production; UGS=underground gas storage; CG=cushion gas; PT=post-treatment; HF=hydraulic fracturing.

RESERVOIR	LOCATION	TYPE	STRESS REGIME	SEISMIC NETWORK	RESERVOIR INFO		
					depth	thickness	production history
Norg	The Netherlands	UGS			2670	140	primary production started in 1983 until 1995 with a max DP of about 117 bar; UGS started in 1995-1997 with a DP for cycle of about 57 bar
Grijpskerk	The Netherlands	UGS			3300	220	primary production started in 1993 until 1994 with a max DP of about 53 bar; UGS started in 1997 with a DP for cycle of about 127 bar
Bergermeer	The Netherlands	UGS	sigma_v = 25 Mpa; sigma_h_min = 9 Mpa (effective stress); initial direction of the minimum horizontal stress is oriented NE-SW	down-hole micro-seismic network	2200	200	primary production started in 1971 until 2006 with a max DP of about 213 bar; no activity between 2007 and 2010; cushion gas injection between 2010 and 2012; UGS started in 2013
Duvernay Formation	Canada	HF	strike-slip regime, oriented at ~45°	regional & local networks	2600-4000	25-60	average mean injection pressure = 62.5 Mpa
Castor	Spain	UGS	graben structure with two families of active faults; the maximum horizontal stress equal to the vertical stress and points to the NE; the minimum horizontal stress equal to 0.7 × vertical stress	Spanish National Network	1800-2000	150-200	initial reservoir pressure = 190 bar; max Dp during primary production = 5 bar. During the injection period the maximum pressure increase observed in the Castor field was 7.6 bar above the initial formation pressure

2.1.1 Norg (The Netherlands)

The fault reactivation and seismic threat in the Norg UGS site is investigated in a NAM technical report (2016). The field lies along a NW-SE trending fault on the west of the Groningen high and is characterized by a structural trapping mechanism. From North to South, the field is compartmentalized in four blocks separated by minor non-sealing faults, while two SW-NE faults bound the reservoir to the North and the South (Figure 1).

Block no. 2 is the block with the highest pressure fluctuations. Along the faults at its boundary two seismic events with magnitude <1.5 have been recorded. The virgin average pressure in Block no. 2 was 327 bar, with a minimum value around 190 bar recorded in 1995. The first seismic event occurred in 1993 during the primary production, while the second one was recorded in 1999 soon after the beginning of the UGS operations.

The original stress regime is affected by some uncertainty. Using density information, the gradient for the vertical stress is estimated at 2.16 bar/10 m at the top of the reservoir. Leak-off tests, properly corrected for reservoir depletion, allowed to quantify in 1.83 bar/10 m the minimum horizontal stress gradient. Available measurements indicate a small difference between the minimum and maximum horizontal stress, between 5% and 10%, with an expected gradient value for the latter equal to 1.92 bar/10 m. The expected orientation for the maximum horizontal stress is 171° East of North, i.e., approximately parallel to the main NW-SE trending fault bounding the reservoir to the west.

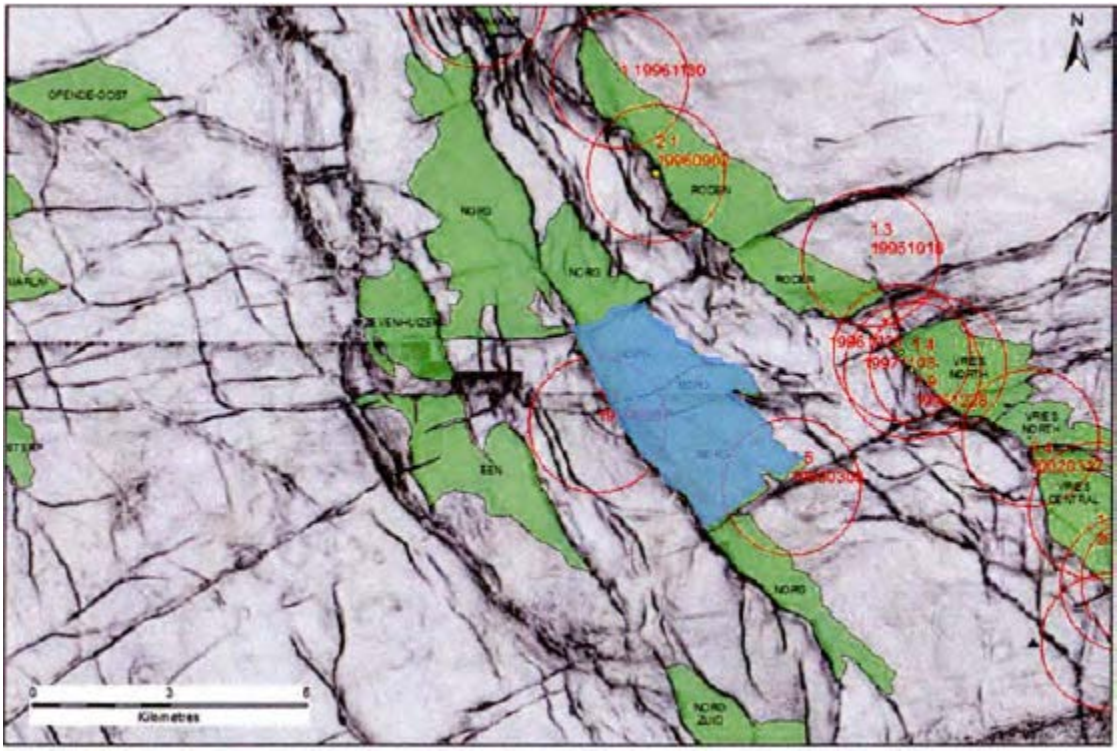

Figure 1 Map of the Norg UGS site (in blue) with traces of the bounding faults and localization of the two recorded seismic events.

The most relevant mechanism for the fault reactivation experienced in the Norg UGS site has been recognized by NAM to be the irreversible stress paths followed by the reservoir during both the primary production and the first injection stage. During the following 17 years, the stress paths mainly developed in the elastic stage and no seismic event has been detected. It has to be observed that the seismic monitoring network implemented until 2016 was not able to record smaller earthquakes, which could have actually occurred.

The NAM report described two 2-D geomechanical models developed to investigate the causes of the two main seismic events. The analyses focus on the role played by the uncertainty on the knowledge of the minimum horizontal stress and by the presence of a thick salt dome above the reservoir. One of the conclusions was that:

"It is found that the presence of salt has a significant impact on the initial stress distribution, and thereby on the potential locations for fault slip. Salt-induced discontinuities in the fault normal stress distribution introduce locations with SCU peak values which may become nucleation points of fault slip and potentially seismic rupture."

For the second seismic event, a role was also played by the variation of elastic properties in the medium and in the fault during the injection stage. In particular, the main cause is found in the reverse shear stress observed after one depletion and re-pressurization cycle, which could have led to a reverse fault slip over a portion of the fault.

2.1.2 Grijpskerk (The Netherlands)

The information on the Grijpskerk UGS is available from previously collected data published in the TNO report (2015). The gas reservoir was produced for few years (1993-1994) and then converted in UGS in 1997. Two seismic events have been detected, the first in 1997 (M=1.3) and the second in 2015 (M=1.5).

The events are connected to the UGS activity even though there are large uncertainties associated with the hypocenter location. Thus, it is not trivial to identify which is the fault or the system of faults activated by the UGS operations. Both events occurred during the production phase at an average pressure of about 280 bar and at a flow rate of 9 million m^3/day. Note that the maximum flow rate operated in the reservoir reached 30 million m^3/day during the production phase in 2013. Although the seismic events occurred at relatively low average pressure (TNO report (2015)), in some wells the pressure equals ~ 200 bar in 1997 and ~ 175 bar in 2015. The average pressure change during UGS cycles is in the range 257-384 bar, but it can locally reach ~ 220 bar, e.g., the GPK-11 or GPK-13 wells in 2015. The sandstone reservoir is ~ 220 m thick and ~ 3300 m deep. As reported by NAM 2010, the caprock is formed by alternating claystone, dolomites, anhydrites and halites, while the underburden consists of claystones and coals.

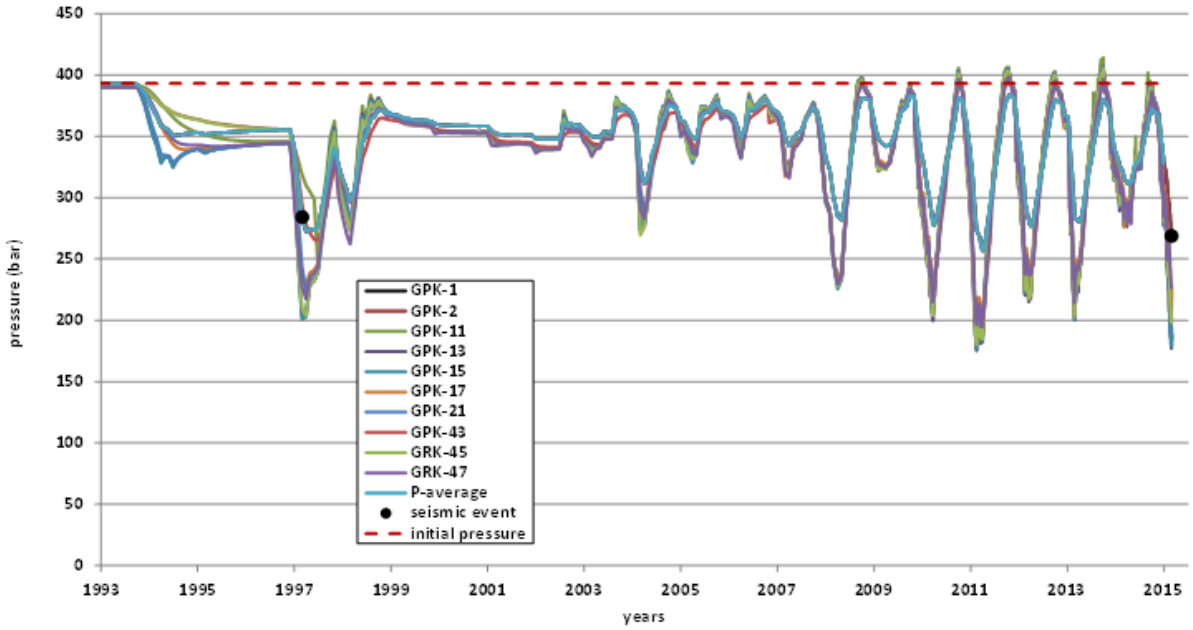

Figure 2 Pressure evolution in time at the Grijpskerk UGS field. The location of the two seismic events in 1997 and 2015 are reported (modified from TNO report (2015)).

2.1.3 Bergermeer (The Netherlands)

The information on the Bergermeer field are available from previously collected data published in the TNO report (2015) and from the publications of Orlic et al. (2013) and Kraaijpoel et al. (2013). The gas reservoir was produced from 1972 to 2007, then shut down for about 3 years until 2010 when it was converted to UGS and cushion gas injection started. The UGS operational volume of 4.1 bcm relies on top of a cushion of 4.6 bcm (Kraaijpoel et al., 2013).

Four seismic events have been detected in 1994 and 2001 during primary production phase. The events are of magnitude in the range 3.0-3.5 and located at the tip of the central fault (TNO report (2015)). The events occurred at an average pressure of 50 bar (1994) and 25 bar (2001). Note that a pressure of 15 bar is reached at the end of production. A downhole micro-seismic monitoring array was installed in 2010 at the underground gas storage site to monitor seismicity induced during storage operations (Kraaijpoel et al., 2013). During injection of cushion gas some small seismic events were detected with a largest magnitude of M=0.7 recorded in 2013 at 75 bar.

The analysis of the micro-seismicity collected over the years 2010-2013 is published in Kraaijpoel et al., 2013 where the following discussion is reported:

"A large fraction of the microseismic events clusters in an area to the east of the central fault tip. In October 2011 a swarm of more than 50 events occurred in that area. 3D-Visualisation revealed that the events line-up along planar surface at a high angle to the central fault. Log correlations and reservoir simulations had already suggested a gas flow baffle in this area that could be associated to a small fault. However, the fault could not be identified on the available 3D seismic. Later reprocessing of the seismic made interpretation of smaller structural elements possible and this small fault could now also be interpreted. The location of the fault is in a small anticlinal curve, in an outer arc extension position. A geomechanical analysis of the effect of this micro faulting indicates that it has a small stabilizing effect on the much larger central fault."

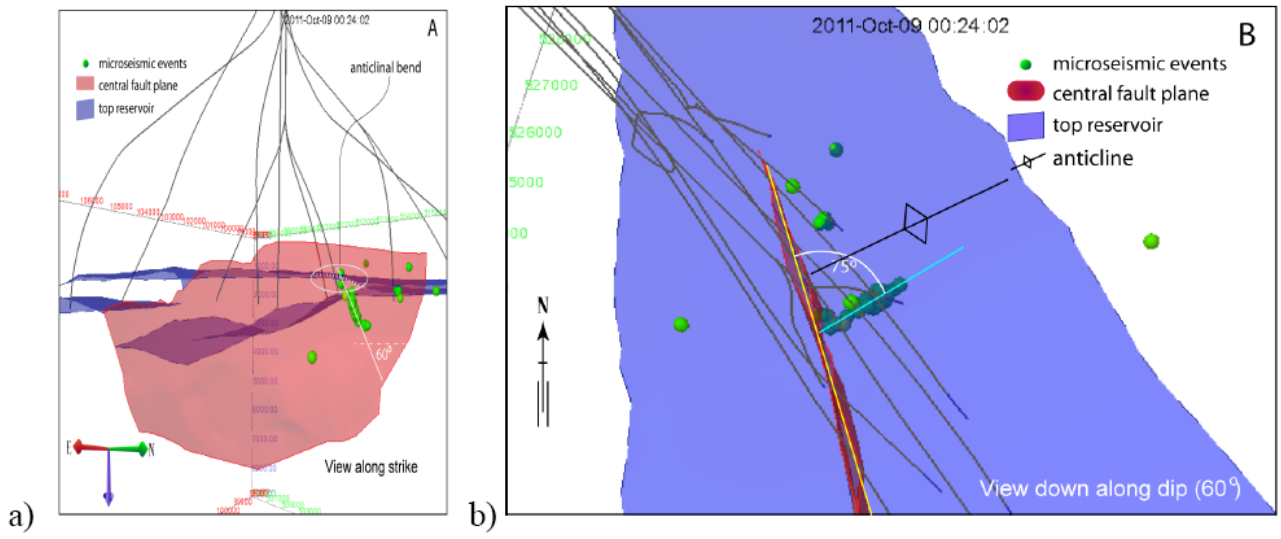

Figure 3 Area of clustered microseismic events (October 2011) in a 3D-Visualisation. The events line-up along a planar surface at a high angle to the central fault (modified after Kraaijpoel et al., 2013).

Thus, according to this analysis and to the geomechanical model results by Orlic et al. (2013), the UGS activity seems to have a stabilizing effect on the central fault. Indeed, Orlic et al. (2013) developed a 3D field scale geomechanical finite element model of the Bergeermer gas field with the following conclusion:

"During annual cycles of gas injection and production, the Central fault is not critically stressed and the predicted stress changes lie in the elastic region. Although the fault slip is unlikely, continuous monitoring of induced seismicity is essential."

2.1.4 Castor (Spain)

Castor is one of the most investigated case study of unexpected induced seismicity. Several publications (both journal papers and internal reports) are available, the most interesting (from our point of view) being Cesca et al. (2014) and Juanes et al. (2017).

Castor is a naturally fractured reservoirs sealed on the west by the Amposta fault. The Amposta fault has been significantly destabilized by injection, with maximum change in Coulomb stress (DCFF) of about 0.5 MPa. According to Juanes et al. (2017), the risk of de-stabilization of a fault is believed to occur for Coulomb stress changes in the order of 0.01 MPa – 0.1 MPa. The initial reservoir pressure was 190 bar and the maximum pressure depletion amounted to 5 bar during primary production. During the injection period the maximum pressure increase observed in the Castor field was 7.6 bar above the initial formation pressure.

Many of the events were triggered on critically stressed, geologically active faults, relieving a component of tectonic stress (Figure 4a). The six largest events in the sequence are clustered along the tectonically active juncture of the Amposta fault and its hanging wall splays (Figure 4b) and occurred wall after the injection closure. Juane et al. (2017) concluded that:

"Presumably, the active portions of the faults were tectonically stressed near the point of failure, and thus Coulomb Force Function changes due to reservoir operations were sufficient to trigger slip."

The locations place these events near the Castor platform. Earthquakes largely occurred on the tectonically active (southern) portion of the Amposta fault and its hanging wall fault splays. Amposta fault is 57°W dip in the vicinity of the field. All of the reservoir faults are steeply (> 45°) east- or west-dipping structures and exhibit normal separation.

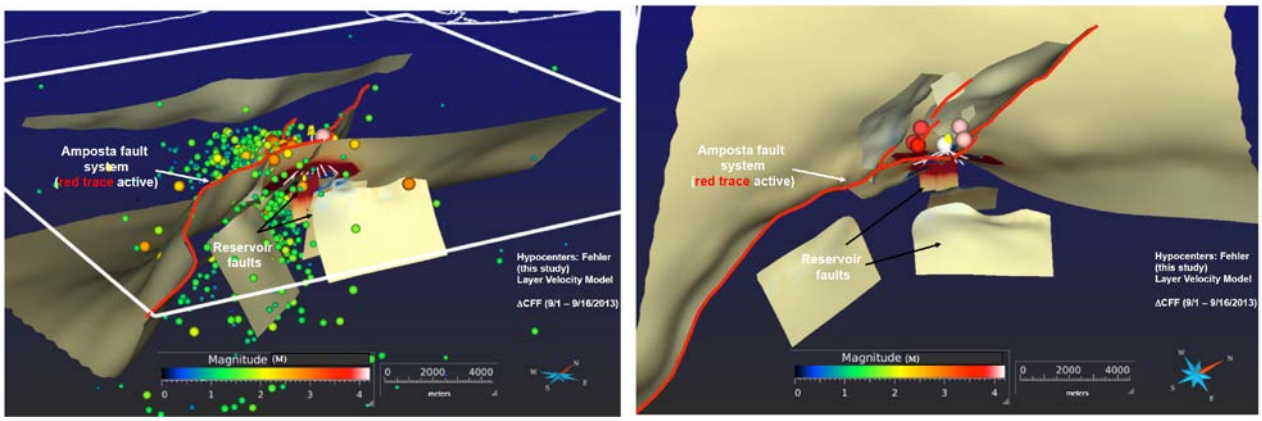

(a) **(b)**

Figure 4 View of the fault systems at Castor with the location of (a) the seismic event recorded between September and October 2013 and (b) the 6 largest earthquakes of magnitude 3.8 to 4.3 recorded in 2013 (after Juanes et al., 2017).

2.1.5 Duvernay Formation (Canada)

Because of well completions, the Duvernay Formation near Fox Creek, Alberta, has experienced some of the largest-magnitude earthquakes related to hydraulic fracturing. The Duvernay Formation is composed of multicyclic units of black organic-rich shale and bituminous carbonates, ranging between 25 and 60 m in thickness. Development of the Duvernay shale-hosted hydrocarbon resources has become economically feasible in recent years, with unconventional operations in the Fox Creek region beginning in June 2010. To date there have been more than 290 horizontal well completions developed in the Duvernay Formation between 2.6 and 4.0 km depth. Average mean pressures, pumping rates, total pumped fluid volume, and proppant weight in well for individual stages are 62.6 MPa, 9.4 m^3/min, 1200 m^3, and 240 t, respectively.

Seismicity within the study region has increased in earthquake rate starting on December 2013. The largest Fox Creek events to date are M ~4 occurred on 23 January 2015, 13 June 2015, and 12 January 2016. The seismic events begin at the level of the Duvernay stimulation interval and extend downward into the shallow Precambrian basement.

Schultz et al. (2017) results suggest that increased pore pressure resulting from Duvernay stimulation is rapidly communicated along the damage zone of mechanically active faults, until reaching a zone of fault weakness (Figure 5, left). Furthermore, during the hydraulic fracturing process pore pressure is stimulated beyond the minimum stress gradient, propagating tensile failures throughout the target rock. These fractures can grow to lengths of up to 500 m vertically. The same authors also note the potential for second-order triggering effects: the adjacent hydraulic fracturing operations have perturbed the ambient stress field, causing the initial fault slip at greater distance (Figure 5, right).

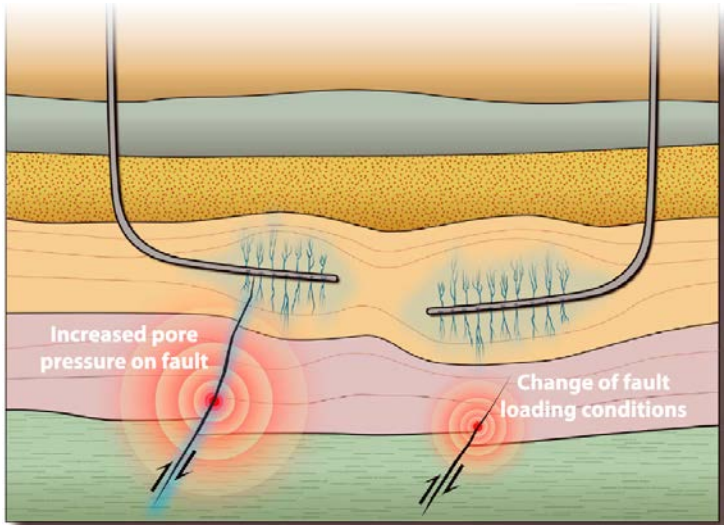

Figure 5 Conceptual diagram which explores two physical mechanisms of initiating slip on a fault as a consequence of hydraulic fracturing. In the left-hand scenario stimulated fracture growth provides hydraulic communication with a preexisting fault. In this case, increased pore pressure on the fault during stage stimulation initiates the fault slip. In the righthand scenario the lateral extent of the completed well is hydraulically isolated from the fault. However, slip can still be initiated on this fault due to stress perturbations associated with mass/volume flux. These perturbations are transmitted poroelastically, during both stimulation and production phases of the well life cycle (after Schultz et al., 2017).

2.2 UGS in Italy

The majority of the UGS plants in Italy are located in the Po river basin (Figure 6). The basin is characterized by shallow marine or deltaic depositional environments with a total sedimentary column that ranges from a minimum of 4–5 km at its northern Alpine border to a maximum of 12 km along the Apennine thrust front. Most of the hydrocarbons detected in the area are Pliocene and Pleistocene biogenetic/diagenetic gas. The Pliocene and Quaternary reservoirs are located in anticlines, thrusted anticlines, simple drape structures, and stratigraphic traps. Gas-bearing rocks range from silty to fine-grained sandstone.

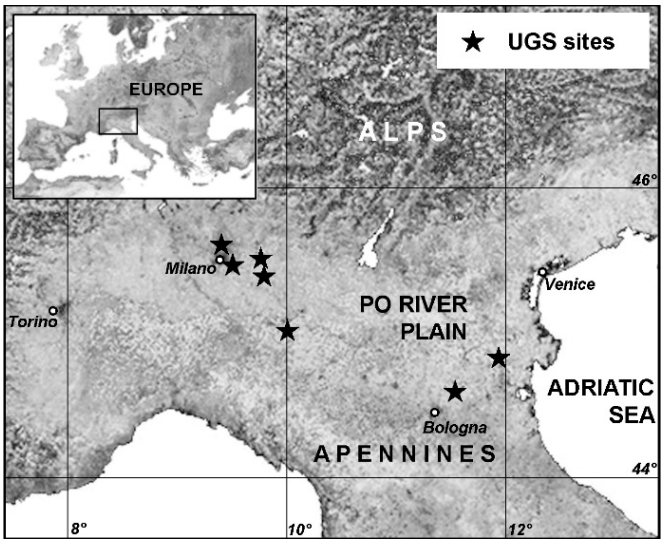

Figure 6 UGS sites in the Po Plain, Italy (after Teatini et al., 2011).

A typical feature of this basin is that gas accumulation occurs in multipay zone reservoirs centimeters to a few tens of meters thick, 1000 to 2000 m deep. Average reservoir porosity ϕ, matrix permeability k, and water saturation S_w range from 25%–30%, 5–1000 mdarcy, and 35%–75% respectively, with net-to-gross pay ratio from 27% in silty sands to 95% in the coarser sands. Reservoirs are sealed on top by deep-marine shales and impermeable sandstone (Mattavelli et al., 1983). A typical geological section and two examples of un-faulted and faulted UGS reservoirs are provided in Figure 7.

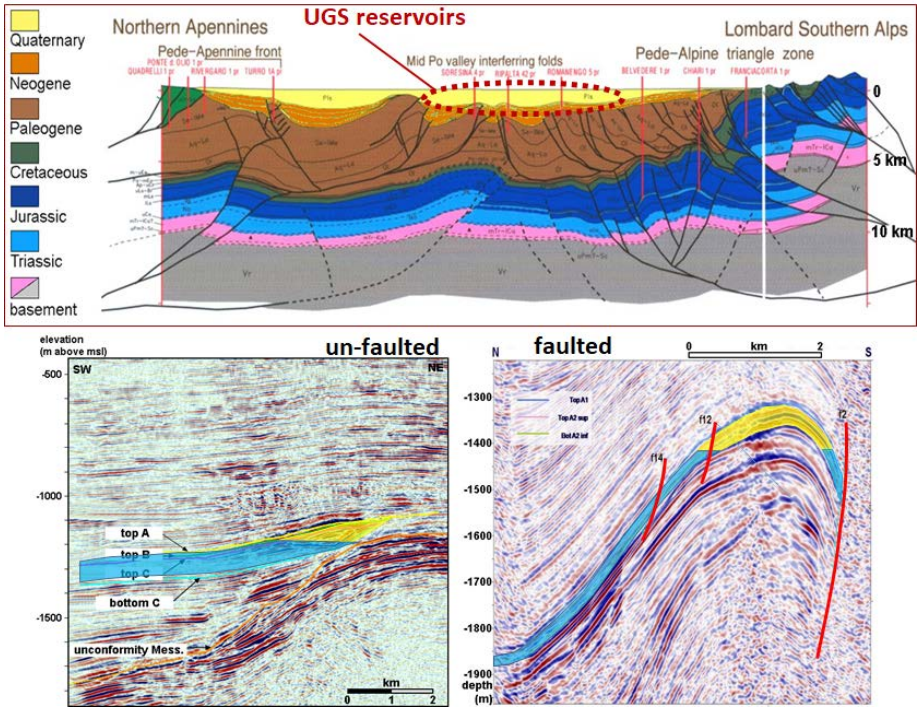

Figure 7 (above) South-west - North-east geologic section of the Po sedimentary basin with the location of the UGS reservoirs. (below) Vertical seismic cross sections through an un-faulted and a faulted UGS gas field in the Po river basin.

The basin is almost normally pressurized and consolidated down to 1000-1500 m depth, with density logs acquired in the basin that provide the following relationship between the total stress σ_z^* (in [bar]) and depth z (in [m]): $\sigma_z^* = 0.12218\,|z|^{1.0766}$. The stress regime in the horizontal directions is highly uncertain and varies with depth (Carminati et al., 2010). In particular, a transition occurs from the shallow tensional / normally consolidated ($\sigma_z > \sigma_H > \sigma_h$) to strike-slip ($\sigma_H > \sigma_z > \sigma_h$) stress field at approximately 1200-1500 m depth and finally to compressional ($\sigma_H > \sigma_h > \sigma_z$) stress field near the main detachment at depth, likely corresponding with the transition from the Pliocene to the Miocene. Regional reverse faults clearly reveal a general compressive stress regime, with the largest horizontal stress σ_H approximately orthogonal to the fault/thrust traces and the smallest σ_h orthogonal to σ_H. From log interpretation, acoustic anisotropy detected by the Sonic Scanner probe, and wellbore ovalization, the direction of the maximal horizontal stress is estimated 18° North.

The pressure evolution versus time follows a similar behavior in all the UGS fields: after a pressure decline of 40 to 80 bar during an approx 10-year primary production, the fields have been converted to UGS, with the pressure that recovers the original value p_i at the end of the cushion gas injection, and a seasonal fluctuation of 30 to 50 bar during UGS cycles, with p_{max} up to 110% p_i (Figure 8).

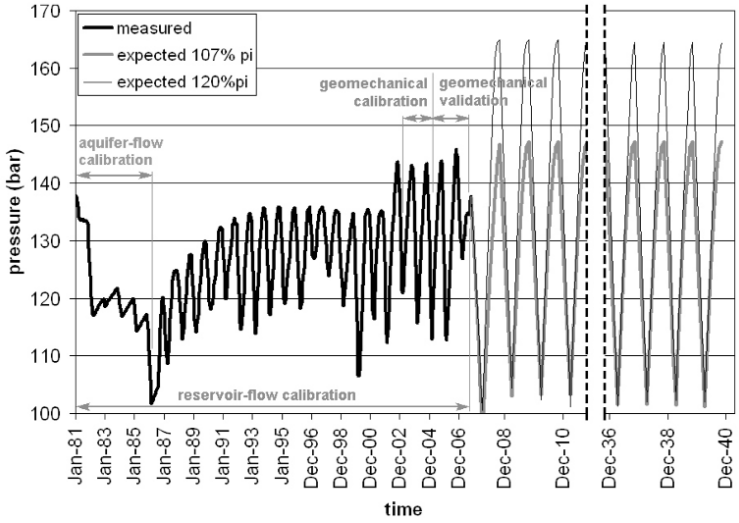

Figure 8 Typical pressure behavior versus time in the UGS gas fields of the Po river basin (after Teatini et al., 2011).

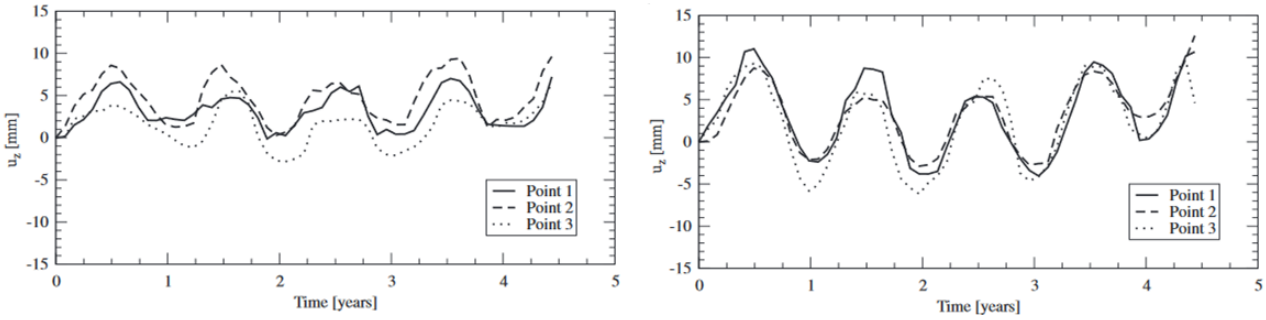

Figure 9 Vertical displacement measured by SAR interferometry above two UGS gas fields in the Po river basin (after Janna et al., 2012).

SAR interferometry has allowed quantifying the displacement above UGS reservoirs since 2002. The available records show a seasonal maximum movement in the range of 5 to 15 mm (Figure 9). It is interesting to notice the elastic behavior of system during the UGS cycles.

This information, together with the interpretation of compaction/expansion records provided by the radioactive marker technique in reservoirs located in the off-shore part of the basin, have allowed to characterize the geomechanical properties of the UGS reservoirs during the primary production (loading, I cycle) phase and the cushion gas injection/UGS (unloading-reloading, II cycle) phase. In loading condition, the following relationship has been developed between the oedometric compressibility c_M (in [bar^{-1}]) and the vertical effective stress (in [bar]): $c_M = 0.01369\ \sigma_z^{-1.1347}$. The ratio between c_M in loading and unloading conditions has been quantified in the range 3 to 5 (Ferronato et al., 2013).

No seismic activity has been linked to UGS activities in Italy till now.

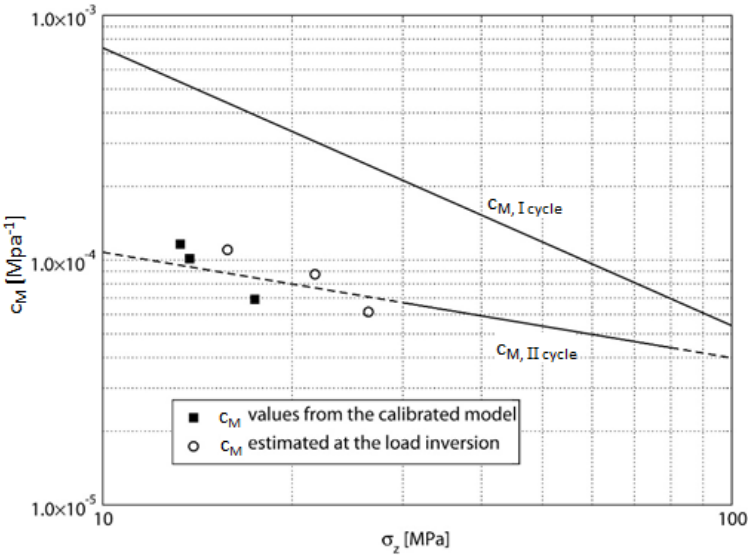

Figure 10 Comparison between vertical compressibility in the Po river basin estimated by radioactive markers and c_M values estimated by calibrating FE geomechanical model to match SAR measurements above UGS fields. Dashed profiles are extrapolations out of its definition range (after Ferronato et al., 2013).

2.3 Other seismic occurrences

The following table (Table 3) summarizes some of the main seismic occurrences recorded during reservoir operations different from UGS activities. Most events are associated to waste water injection and geothermal fluid production. The mechanisms activated in these projects are likely to be different from those encountered in UGS plants. Nonetheless, the examples that follow are reported for the sake of completeness.

RESERVOIR	LOCATION	TYPE	ACTIVATED FAULT GEOMETRY			DEPTH (m)			MAGNITUDE			STRESS REGIME	SEISMIC NETWORK	RESERVOIR INFO	
			strike	dip	rake	below	reservoir	above	≤1	1 - 3	≥3			depth (m)	production history
Geysers	California (USA)	W_inj	N135E			x (3500 - 4000)					x	SH N60E (theta = 30, M1 = 1, M2 < M1)	micro-seismic network in deep wells	2500	Water Injection (geothermal field) from 1960
Prague	Oklahoma (USA)	W_inj	N30E			x (3500 - 4500)					x	SH N70E > Sv > Sh	Oklahoma geological survey	2500	Flowback water injection from 2009
Guy	Arkansas (USA)	W_inj	N30E			x (4000 - 6000)					x	SH N60E	seismic stations WHAR	2000	Flowback water injection from 2009
Basel	Switzerland	W_inj	N30E				x				x	SH N135E	micro-seismic network in deep wells	4000	Water Injection (geothermal field) in 2006. Max DP of about 300 bar
Soult-sous-Forêts	France	W_inj	N20E	135			x			x		SH N160E	micro-seismic network in deep wells	5000	Water Injection (geothermal field) from 2000. Max DP of about 150 bar
Fox Creek	Alberta (Canada)	W_inj	N0E			x (3750)					x	SH N45E	local broadband seismographic stations	3500	Hydraulic fracturing from 2013
Val d'Agri	Italy	W_inj	N135E	45 (+180)		x (4500)				x		Sh N45E ?	INGV permanent stations	3000	Waste water injection from 2006. Max DP of about 100 bar
Habanero	Australia	W_inj	190	20	100		x			x		SH N80E	local broadband seismographic stations	4000	Water Injection (geothermal field) from 2002 to 2012. Max DP of about 400
Lacq	France	Gas production	100	100			x				x	no info	IPGS and LGIT seismographic stations	4000	Gas production started in 1957 and it stopped in 2008. Max DP of about 600 bar

References

Carminati, E., D. Scrocca, and C. Doglioni (2010), Compaction-induced stress variations with depth in an active anticline: Northern Apennines, Italy, J. Geophys. Res. - Solid Earth 115 B02401 doi: 10.1029/2009JB006395.

Cesca S., et al. (2014). The 2013 September–October seismic sequence offshore Spain: a case of seismicity triggered by gas injection? Geophys. J. Int., 198, 941–953.

Ferronato, M., N. Castelletto, G. Gambolati, C. Janna and P. Teatini (2013). II cycle compressibility from satellite measurements, Geotechnique, 63(6), 479-486, doi:10.1680/geot.11.P.149.

Janna, C., N. Castelletto, M. Ferronato, G. Gambolati and P. Teatini (2012). A geomechanical transversely isotropic model of the Po River basin using PSInSAR derived horizontal displacement, Int. J. Rock Mech. Mining Sci., 51, 105-118.

Juanes R., et al. (2017). Coupled flow and geomechanical modelling, and assessment of induced seismicity, at the Castor underground gas storage project – Final Report, 86 pp.

Kraaijpoel D.A., Nieuwland D.A. and Dost B. (2013). Microseismic Monitoring and Subseismic Fault Detection in an Underground Gas Storage, 4th EAGE Passive Seismic Workshop, DOI: 10.3997/2214-4609.20142354.

Mattavelli, L., T. Ricchiuto, D. Grignani, and M. Schoell (1983), Geochemistry and habitat of natural gases in Po Basin, Northern Italy, AAPG Bull., 67(12), 2239–2254.

NAM, 2010. Update opslagplan Grijpskerk, November 2010.

NAM, 2016. Norg UGS fault reactivation study and implications for seismic threat. October, 2016.

Orlic B., Wassing B.B.T., and Geel C.R. (2013). Field Scale Geomechanical Modeling for Prediction of Fault Stability During Underground Gas Storage Operations in a Depleted Gas Field in the Netherlands, American Rock Mechanics Association, 47th U.S. Rock Mechanics/Geomechanics Symposium, 23-26 June, San Francisco, California.

Schultz, R., R. Wang, Y. J. Gu, K. Haug, and G. Atkinson (2017). A seismological overview of the induced earthquakes in the Duvernay play near Fox Creek, Alberta, J. Geophys. Res. Solid Earth, 122, 492–505, doi:10.1002/2016JB013570.

Teatini, P., N. Castelletto, M. Ferronato, G. Gambolati, C. Janna, E. Cairo, D. Marzorati, D. Colombo, A. Ferretti, A. Bagliani and F. Bottazzi (2011). Geomechanical response to seasonal gas storage in depleted reservoirs: A case study in the Po River basin, Italy, J. Geophys. Res., 116, F02002, doi:10.1029/2010JF001793.

TNO 2015 R10906 - Injection-Related Induced Seismicity and its relevance to Nitrogen Injection: Description of Dutch field cases.